

The Effect of Mechanical State on the Equilibrium Potential of Alkali Metal/Ceramic Single-Ion Conductor Systems

Eric A. Carmona, Michael J. Wang, Yueming Song, Jeff Sakamoto, and Paul Albertus*

The relationship between mechanical stress states and interfacial electrochemical thermodynamics of Li metal/Li_{6.5}La₃Zr_{1.5}Ta_{0.5}O₁₂ and Na metal/Na-β"-Al₂O₃ systems are examined in two experimental configurations with an applied uniaxial load; the solid electrolytes are pellets and the metal electrodes high-aspect-ratio electrodes. The experimental results demonstrate that 1) the change in equilibrium potential at the metal/electrolyte interface, when stress is applied to the metal electrode, is linearly proportional to the molar volume of the metal electrode, and 2) the mechanical stress in the electrolyte has a negligible effect on the equilibrium potential for an experimental setup in which the electrolyte is stressed and the electrode is left unstressed. Solid mechanics modeling of a metal electrode on a solid electrolyte pellet indicates that pressure and normal stress are within ≈0.5 MPa of each other for the high aspect ratio (≈1:100 thickness:diameter in our study) Li metal electrodes under loads that exceed yield conditions. This work should aid in advancing the quantitative understanding of alkali metal dendrite formation within incipient cracks and their subsequent growth, and pore formation upon stripping, both situations where properly accounting for the impact of mechanical state on the equilibrium potential is of critical importance for calculating the current distribution.

1. Introduction

Replacement of the conventional graphite anode with lithium metal would enable increased energy content on gravimetric (≈35%) and volumetric (≈50%) cell-level bases and the potential for manufacturing cost reduction; however, the development and adoption of rechargeable lithium metal batteries (LMBs)


face challenges.^[1] In conventional organic liquid electrolytes, lithium is prone to irreversible capacity loss due to side reactions and the formation of dendritic protrusions that can lead to shorting, cell failure, and potentially fires.^[2,3] Solid electrolytes have been proposed as a means of mitigating these issues and achieving desired cycling characteristics for LMBs.^[4] A number of groups have studied the electrochemically active interface between alkali metals and solid-state electrolytes, the influence of stresses on battery performance, and electrochemically induced expansion of electrode materials.^[5–9] Despite the investigation of various solid electrolytes including polymers, oxides, sulfides, and more, none have yet been shown capable of preventing dendrite formation and cell failure while demonstrating all commercially desired performance and cycling characteristics for vehicle applications.^[10–12]

Characterizing the thermodynamic and kinetic states at the lithium/electrolyte interface is essential for understanding

lithium plating and stripping because they affect the current distribution over the electrode surface and thereby determine whether initiation sites grow into dendrites that lead to shorting. Mechanical work done on or by a material system changes the Gibbs free energy of that material system. For fluids (especially compressible fluids), pressure-volume work is typically used, whereas for solid materials (especially those that undergo elastic deformations, requiring use of the Cauchy stress tensor) stress-displacement work is used. When considering the effect of mechanical state on electrode and electrolyte thermodynamic states, the stress and molar volume (for a pure phase) or partial molar volume (for a variable composition phase) determine changes in Gibbs free energy. In the literature, there are several proposed models assessing how stress distributions at a lithium electrode/electrolyte interface impact the interfacial thermodynamics and kinetics; however, there are discrepancies regarding which stresses to use and whether the mechanical state of the electrolyte impacts the equilibrium potential. Newman and Monroe developed a model to assess the effect of interfacial deformation on reaction kinetics and thermodynamics at a metal electrode with a polymer electrolyte in which a salt concentration gradient can develop (e.g., PEO).^[13] Starting from thermodynamic relationships, they obtained an expression for the change in electron chemical potential caused by a

E. A. Carmona, Dr. Y. Song, Prof. P. Albertus
Department of Chemical and Biomolecular Engineering
University of Maryland
College Park, MD 20742, USA
E-mail: albertus@umd.edu

Dr. M. J. Wang, Prof. J. Sakamoto
Department of Materials Science and Engineering
University of Michigan
Ann Arbor, MI 48109, USA
Prof. J. Sakamoto
Department of Mechanical Engineering
University of Michigan
Ann Arbor, MI 48109, USA

 The ORCID identification number(s) for the author(s) of this article can be found under <https://doi.org/10.1002/aenm.202101355>.

DOI: 10.1002/aenm.202101355

change in pressure in both the electrode and electrolyte. They used an interfacial stress balance to obtain the pressure and deviatoric stresses present in both the electrode and electrolyte, and subsequently how these mechanical states affect the kinetics and thermodynamics of a reaction at the interface.^[13] Pannikkat and Raj studied the stress induced change in equilibrium potential between two platinum electrodes (one stressed, one unstressed) with yttria-stabilized zirconia electrolyte at elevated temperatures.^[14] Uniaxial compression was applied to a working electrode on the top of a sample of Y_2O_3 - ZrO_2 , with an unstressed reference electrode on the side of the sample. These authors posited that the change in equilibrium potential due to applied stress was related to the normal stress at the interface, rather than pressure and deviatoric stresses, and that for their system only the mechanical state of the solid electrolyte affected the equilibrium potential. The experimental geometry used by Pannikkat and Raj, as well as a gas-phase reactant (O_2), leads to challenges applying their results to metal electrode systems, but it is an early experimental work addressing stress-potential coupling. More recently, Ganser et al. developed a version of the Butler-Volmer equation considering mechanical states for a variety of electrolyte and electrode systems using transition state theory.^[15] For a system composed of a binary electrolyte in a solvent and a metal electrode, they developed a kinetic expression comparable to Newman and Monroe's. For this case, the change in equilibrium potential due to mechanical stress at the interface is given by,

$$V_{eq} = \frac{1}{F} (\Delta G_{Ref} + \Omega_M \sigma_n^M + \Omega_+ p_n^+) \quad (1)$$

Here, V_{eq} is the equilibrium potential between the electrode and electrolyte at the interface, ΔG_{ref} is the reference difference in Gibbs free energies between the electrode and electrolyte, σ_n is the applied normal stress, Ω is the molar or partial molar volume, script M denotes the metal electrode, the script + denotes the ion in the electrolyte, and p refers to the pressure. They state that the pressure can be substituted for the normal stress in the case of a weak solid (which we interpret to mean a solid with a yield strength significantly lower than the applied or generated stresses), because once a solid yields, the pressure and normal stress are of negligible difference in a weak material (just as it is for a fluid without any yield stress). For a single-ion conductor with a metal electrode, Ganser et al. posited that only the mechanical state of the electrode affected the thermodynamic state and kinetics of the reaction,^[15]

$$V_{eq} = \frac{1}{F} (\Delta G_{Ref} + \Omega_M \sigma_n) \quad (2)$$

An analogous expression is used in the work of Barroso-Luque et al. who also modeled a metal electrode with a single-ion conductor; however, the pressure is substituted for the normal stress in the work of Barroso-Luque et al., demonstrating potential discrepancies in the literature regarding the mechanical state in the electrode that determines the interfacial thermodynamic states.^[16]

Mistry and Mukherjee also modeled the effect of mechanics on Li deposition with a metallic lithium electrode and solid

single-ion conducting electrolyte.^[17] In their model, they propose that the equilibrium potential is a function of the mechanical state of both electrode and electrolyte similar to Equation (1) above, and they use hydrostatic stress (i.e., pressure) as the stress term. They conclude that an increased disparity between Ω_{Li} and Ω_{Li+} leads to a reaction bias favoring localized deposition. We note that several uses and definitions of the partial molar volume of Li^+ in a solid ion conductor (e.g., LLZO) can be found.^[17-19] Some authors treat Ω_{Li+} as zero, as the lithium cations are part of the crystal lattice structure and cannot undergo addition or removal without affecting charge neutrality,^[18] while others describe the partial molar volume of an ion in a crystalline solid electrolyte as the volume of the ion in the crystal, subject to certain definitions.^[19] We prefer to retain the definition of the partial molar volume of a species as $(\partial V / \partial n_i)_{T,P,n_j \neq i}$ because of its clear ability to be measured experimentally. Because $Li_{6.5}La_3Zr_{1.5}Ta_{0.5}O_{12}$ (LLZO) and $Na-\beta'-Al_2O_3$ (NBA) are not variable-composition materials (i.e., they don't develop internal spatial compositional variations during battery cycling), the partial molar volume of Li^+ (for LLZO) and Na^+ (for NBA) in these materials is not defined.

In this work, we use experiments and models to investigate how mechanical stresses affect the equilibrium potential of two alkali metals/single-ion conducting electrolyte interfaces. In particular, we provide the first direct thermodynamic measurements of how stress, and which type of stress, affects the equilibrium potential of both Li and Na metals and single-ion conducting solid electrolytes. We address the questions of whether pressure or normal stress is the correct quantity for assessing the effect of mechanics on the equilibrium potential, and if the mechanical state of the solid electrolyte, electrode, or both affect the equilibrium potential.

2. Experimental Section

2.1. Materials Synthesis and Cell Assembly

LLZO of the composition $Li_{6.5}La_3Zr_{1.5}Ta_{0.5}O_{12}$ and $Na-\beta'-Al_2O_3$ were synthesized and densified to relative densities >95% as described in previous works.^[20,21] The electrolytes were ground and polished with progressively finer grits with a final polish using a 1 μm diamond paste.

To deposit the Li metal, the LLZO surfaces were masked with laser-cut polyamide and then 20 μm of Li was deposited using a thermal vapor deposition system (Angstrom Engineering). The polyamide masks were then removed, leaving 2 mm diameter Li pads to act as the working and reference electrodes as shown in Figure 1a. To deposit Na metal onto the NBA surface, Na metal (Sigma Aldrich) was cold-rolled and punched into 2 mm diameter foils and placed on the NBA surface in the same configuration as Figure 1a. For both systems, the electrolytes are heat-treated in Ar at 400 °C for LLZO and 700 °C for NBA to remove contamination layers from the electrolyte surfaces. To minimize the deformation of the Na foil during the actual experiments (due to the low yield stress of Na and the relatively large thicknesses of the foil), prior to experiments, the Na foils were compressed with a force of 100 N for 1 h such that the diameter of the working electrode increased to a final diameter

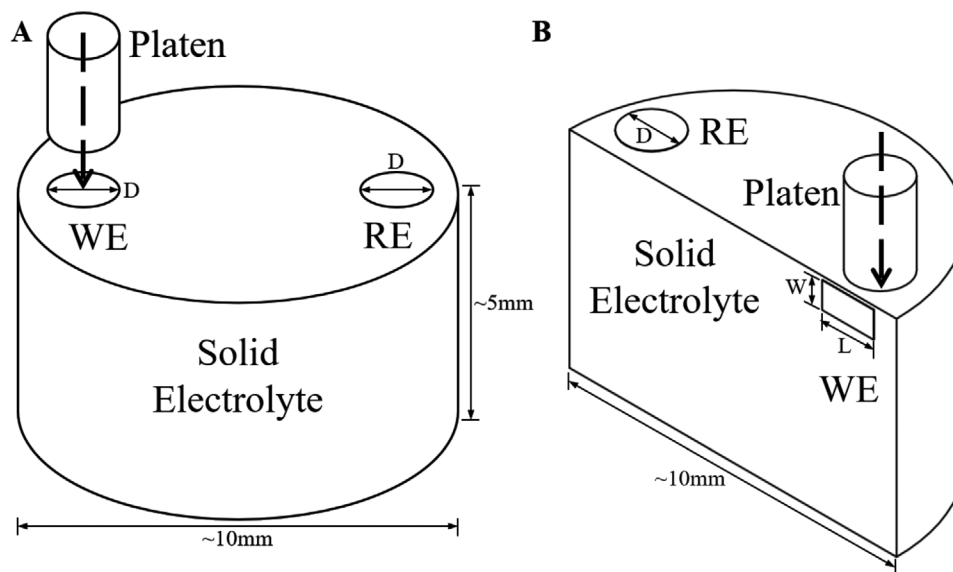


Figure 1. Schematic of Experimental Setups. a) The platen applies a normal compressive stress to the working electrode/solid electrolyte interface. Both Na/NBA and Li/LLZO material systems were studied for this setup. D is the initial diameter of the WE and RE, 2 mm for Li and ≈ 3.5 mm for Na. b) In this setup the platen applies a compressive stress to LLZO, and the Li WE is present on a face perpendicular to the top plane. W is the width of the lithium WE, 1 mm, and L is the length of the WE, 2 mm.

of ≈ 3.4 to 3.7 mm. To measure the effect on the equilibrium potential of an applied stress on the LLZO but not the working electrode, the configuration in Figure 1b was used. In this configuration, the LLZO was cut to create a flat face perpendicular to the top plane. The reference electrode was deposited as in Figure 1a, and then the working electrode was deposited using the same thermal vapor deposition method onto the perpendicular face.

2.2. Electrochemical Measurements

An Instron 5944 compression/tension unit housed inside an Ar-filled glovebox was used to control the applied stress while a Bio-logic VMP300 was used to measure the electrochemical potential. To apply stress to the working electrode, a custom Ni-coated stainless-steel platen was used. The face of the platen was polished to a mirror finish with P2500 sandpaper to minimize roughness-induced stress concentrations. A tungsten probe was used to contact the reference electrode. In the configuration of Figure 1a, the platen was used as the current collector to the working electrode while in Figure 1b, a second tungsten probe was used.

For the Li/LLZO system, the open-circuit potential was measured for 1 h at each stress with force increments of 50 N. For LLZO, the upper-bound of the applied force was limited by fracture of the LLZO, which is expected to occur at ≈ 100 MPa. As demonstrated by Barosso-Luque et al., >100 MPa stresses can potentially be generated within a ceramic solid electrolyte crack tip prior to fracture.^[16] For the Na/NBA system, significantly more deformation of the Na metal due to yield and creep were expected and therefore the force was only incremented by 10 N between each measurement, to minimize changes in the applied true stress during the experiments. Additionally, to

minimize the time of the experiment and therefore the deformation induced, the potential was only measured at each force for 5 min.

2.3. Mechanics Simulations

Equilibrium stress distributions for each experimental setup were calculated using the finite element package COMSOL Multiphysics, the Structural Mechanics module, and the Non-linear Structural Mechanics module. The mechanical properties used in the simulations are summarized in Table 1, both configurations in Figure 1 were modeled, but only for the Li metal/LLZO material system. For the experimental configuration shown in Figure 1a, the solid electrolyte pellet was modeled with a diameter of 10 mm and a thickness of 5 mm. The Li electrodes were modeled with diameters of 2 mm and thicknesses of 20 μm . A fixed boundary condition was applied to the bottom boundary of the solid electrolyte pellet, and a boundary load was applied to the top of the Li working electrode. The platen/electrode, electrode/electrolyte interfaces, and edges of the electrode were prescribed no displacement conditions in the radial (x - and y -directions) direction. A logarithmic sweep

Table 1. Mechanical Properties used in Li/LLZO equilibrium stress calculations. Li properties^[13] and LLZO properties.^[22]

Name	Quantity	Unit
Li metal Poisson's ratio	0.42	–
Li metal Shear modulus	3.4	GPa
Li metal yield strength	0.7	MPa
LLZO Poisson's ratio	0.26	–
LLZO Shear modulus	60	GPa

of boundary loads from 0 to 100 MPa was conducted. For the experimental configuration shown in Figure 1b, a no displacement boundary condition was applied at the bottom boundary of the solid electrolyte pellet, and a boundary load was applied where the platen contacts the solid electrolyte. All other boundaries were treated as free.

3. Results and Discussion

The experimental setups for measuring the stress-induced potentials are illustrated in Figure 1. To correlate the equilibrium potential with the applied stress, LLZO, and NBA were used as two model electrolyte systems. To measure the effect on the equilibrium potential of an applied stress on the LLZO but not on the working electrode, the configuration shown in Figure 1b was used.

The results acquired using the experimental configuration in Figure 1a are summarized in Figure 2. Figure 2a,c depict the transient potential measured between the stressed working electrode and the unstressed reference electrode (in the study, the reference electrode served as the counter electrode) with the corresponding applied normal stress. Figure 2b,d demonstrate the linear relationship between measured potential and applied stress for each of the three trials conducted for each material set.

Equation (2) indicates that $\Delta\phi$ versus applied stress should have a linear relationship, pass through the origin, and have a slope equal to the molar volume of the metal electrode divided by F . Using Equation (2) and the fit for the Li/LLZO system shown in Figure 2b, the molar volume of Li from regression, $12.23 \text{ cm}^3 \text{ mol}^{-1}$, is within 6% of the actual value of $13.0 \text{ cm}^3 \text{ mol}^{-1}$. For Na/NBA and the fit shown in Figure 2d, the

molar volume of Na from regression, $22.51 \text{ cm}^3 \text{ mol}^{-1}$, is within 5.5% of the actual value, $23.78 \text{ cm}^3 \text{ mol}^{-1}$. The molar volume of a solid is a function of pressure; however, the influence of pressure on the molar volume should be on the order of 1% or less in our case. These results are in close agreement with Ganser's model for a metal electrode and a single-ion conducting electrolyte; changes in potential with stress are proportional to the molar volume of the metal electrode, with no apparent effect due to the electrolyte.^[15] To our knowledge, these are the first careful measurements of this effect with well-defined geometries and careful attention to all experimental aspects for Li and Na metal electrodes with ceramic single-ion conducting electrolytes. This is an important result worth reiterating: for this configuration, the mechanical state of the electrolyte appears to have a minimal (i.e., <5% of the overall equilibrium potential response to an applied stress) effect on the equilibrium potential of the reaction.

To better understand the full state of the stress, COMSOL was used to simulate the stress distributions in the working electrode and electrolyte for the configurations in Figure 1a,b. In particular, these simulations were used to determine the normal stress and pressure distributions at the stressed electrode/electrolyte interface. The Li metal electrode was treated as linear elastic followed by perfectly plastic material once the Von Mises stress exceeded the yield strength. Modeling Li as perfectly plastic was chosen due to its lack of work hardening at the strain rates and temperature of these experiments.^[23,24] The LLZO was treated as a linear elastic material; it does not have a well-defined yield strength or exhibit ductile deformation. Figure 3 shows the pressure and normal stress distributions in the Li working electrode at the electrode/electrolyte interface for the experimental setup in Figure 1a.

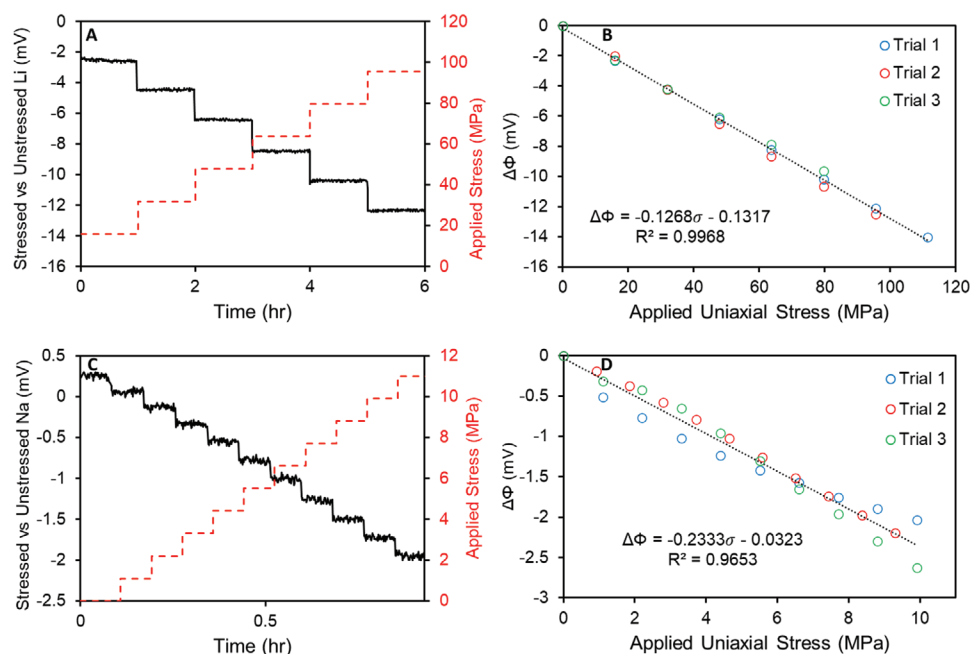


Figure 2. Measured equilibrium potential as a function of applied stress. a) Transient stress-induced potential for Li electrodes with LLZO electrolyte. b) Multiple trials of steady state stress induced potential for Li electrodes with LLZO electrolyte with regression. c) Transient stress-induced potential for Na electrodes with NBA electrolyte. d) Multiple trials of steady state stress induced potential Na electrodes with NBA electrolyte with regression. $\Delta\phi$ is defined as the measured potential between the working and reference electrodes minus the potential at an applied stress of 0 MPa.

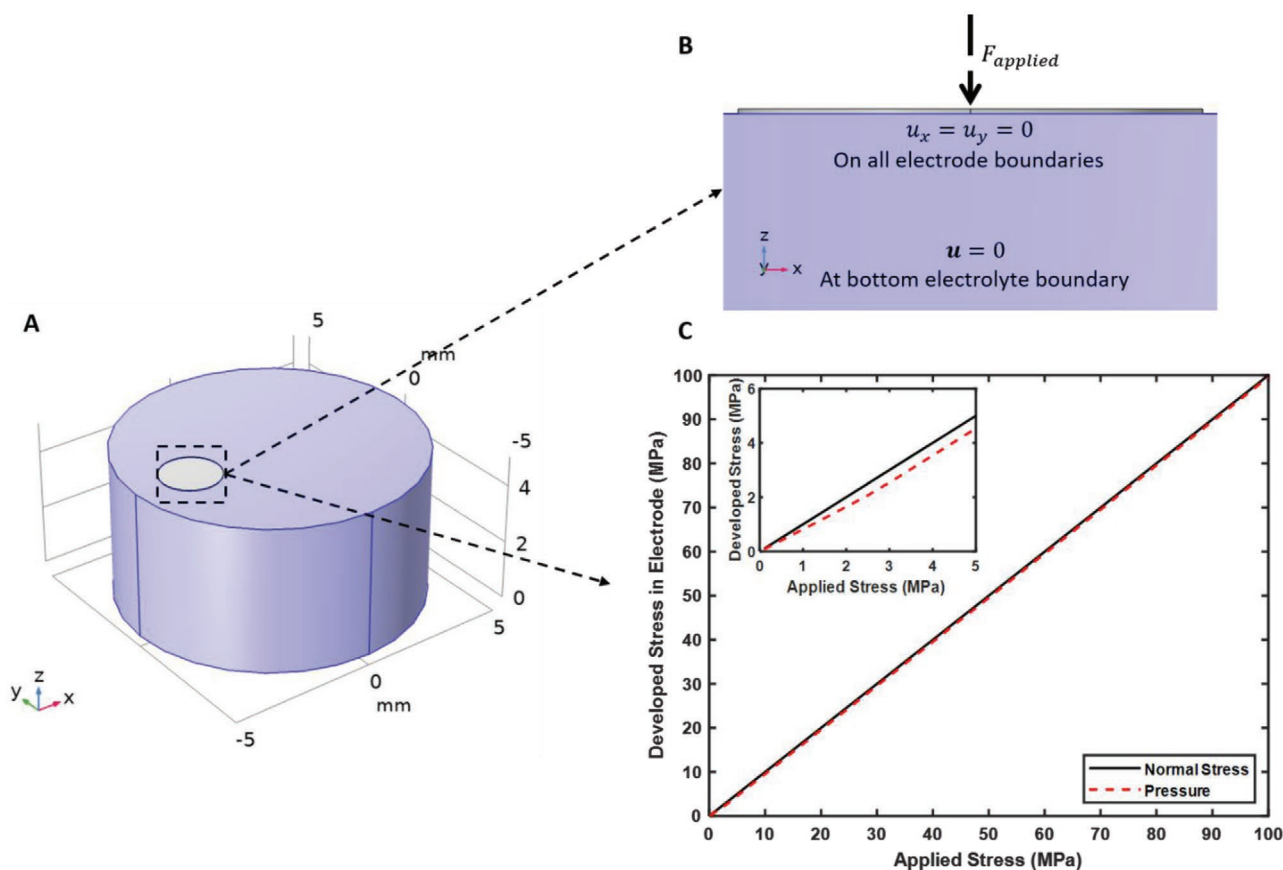


Figure 3. COMSOL Model of Experimental Configuration 1a for Li/LLZO. a) Schematic of modeling domain for experimental configuration 1a. b) Boundary conditions at the electrode/electrolyte interface. c) Developed Normal Stress and Pressure in the electrode as a function of the Applied Stress.

No slip boundary conditions were applied at the electrode/platen and electrode/electrolyte interfaces, only allowing displacement in the z-direction at these interfaces. The edges of the Li electrode were also constrained to movement in only the z-direction. These conditions were selected due to the high friction developed at these interfaces, leading to hydrostatic pinning.^[25] In our model, the Li yields once the Von Mises stress exceeds the yield strength at an applied load of ≈ 2.6 MPa; however, the friction at the two interfaces coupled with the high aspect ratio of the electrode limits observable radial flow of the Li to time scales exceeding that of our experiments, justifying our selection of fixed boundaries on the electrode edges. Masias et al. observed increasing flow stress with decreasing aspect ratio (diameter:thickness in their study) for mineral oil lubricated Li and platens; we expect the friction and adhesive forces in our experiment to be greater due to the unlubricated Li/platen and vapor deposited Li/LLZO interfaces, resulting in more hydrostatic pinning than was observed in their work. From Figure 3, after plastic deformation occurs, the normal stress in the Li and the pressure are nearly equal, differing by ≈ 0.5 MPa. This offset corresponds to a difference of ≈ 0.06 mV in the stress induced potential (using the slope in Figure 2b), a value that will be difficult to observe experimentally.

Our model of the Li electrode in the configuration in Figure 1a is confining the volume of the metal electrode on the sides and bottom, but when it is compressed from the top, it

will first develop stresses according to elastic mechanics. Once the Von Mises stress is exceeded, the Li metal will yield, and the components of the Cauchy stress tensor will satisfy the Von Mises yield criterion for a material under principal stresses. Our model shows that at $\approx 1:100$ aspect ratio (thickness:diameter), Li (and we can infer Na) will yield at applied normal stresses of a few MPa at most, and once that happens, pressure and normal stress are negligibly different compared to the magnitudes of applied normal stress. This is before considering the significant rates of room-temperature creep, so for the treatment of sodium and lithium metal electrodes at temperatures of 25 °C and higher, the pressure and normal stress can be used interchangeably within a corresponding electrochemical accuracy of < 0.1 mV.

To further investigate whether an applied stress affects the equilibrium potential at a single-ion conducting solid electrolyte/metal electrode interface, we performed experiments using the configuration depicted in Figure 1b, and we show the results in Figure 4. To our knowledge, this is the first attempt to directly measure whether the mechanical state of a single-ion conductor affects the equilibrium potential at a metal electrode interface.

The voltage transient in Figure 4a, and time-averaged results for each of three trials shown in Figure 4b, indicate that stress in the electrolyte alone leads to a < 0.5 mV change in potential between the electrodes. We also note that the magnitude of any

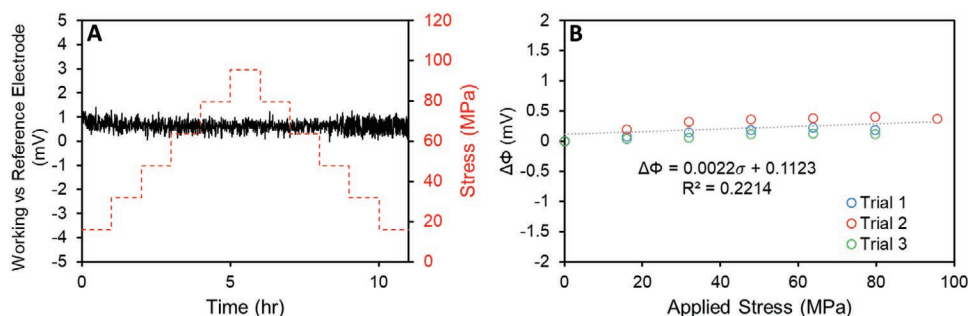


Figure 4. Potential difference between unstressed lithium electrodes with a stressed electrolyte according to the setup in Figure 1b. a) Voltage transient with step changes in applied stress on LLZO. b) Measured potential for multiple trials. Here, the potential is averaged over the hour spent at each stress.

signal in Figure 4b is within the noise shown in the transient in Figure 4a. This is additional experimental evidence that the mechanical state of the metal electrode is the most important quantity affecting the equilibrium potential for ceramic, single-ion conducting electrolytes.

To further understand the mechanical state at the interface of the Li electrode and LLZO electrolyte, **Figure 5** shows equilibrium stress calculations that indicate pressures $\approx 8\times$ larger are developed in the electrolyte compared to the Li electrode. The pressure values in Figure 5b are surface averages at the interface, as the pressure varies significantly across the interface due to the stress distribution that results from experimental geometry and boundary conditions. We are showing pressure rather than normal stress (x -direction) because the normal stresses developed at the interface are effectively zero due to the free boundary at the Li/LLZO interface. The pressure is non-zero primarily due to the stress in the z -direction. There are significant complexities associated with designing an experiment with normal stresses developed only in the electrolyte. For the LLZO electrolyte studied here, our hypothesis is that its mechanical state does not affect the equilibrium potential for several possible reasons, including 1) there is no volume change associated with passing ionic current because of the conduction mechanism, 2) the chemical potential of Li^+ may be a weak function of stress applied to the entire LLZO phase.

4. Conclusion

This study examines the change in equilibrium potential as a result of applied mechanical stress for two metal electrode/single-ion conducting solid electrolyte systems. The two key experimental contributions from this work include 1) the first careful measurements of how applied stress on Li and Na metal electrode against a solid electrolyte affects equilibrium potential, 2) the first attempts to directly measure whether an applied stress on an electrolyte affects the equilibrium potential. Regarding (1), our experiments demonstrate that the equilibrium potential is proportional to the molar volume of the metal electrode and the applied stress. Regarding (2), our experiments show that stresses in the single-ion conducting solid electrolytes studied here have negligible effect on the interfacial thermodynamic state. In addition to experimental work, we modeled the equilibrium stress distributions for two experimental platforms. For uniaxial compression to well above yield conditions for Li metal, we found that the normal stress and pressure values in the electrode are within ≈ 0.5 MPa, leading to a negligible difference in potential, ≈ 60 μV , indicating the use of p and σ_n are interchangeable for high aspect ratio electrodes (1:100 in this case) under loads generating a Von Mises stress exceeding the yield strength. Hydrostatic pinning due to the frictional and adhesive forces at the electrode/platen and electrode/electrolyte interfaces prevent flow of the metal electrode and cause the

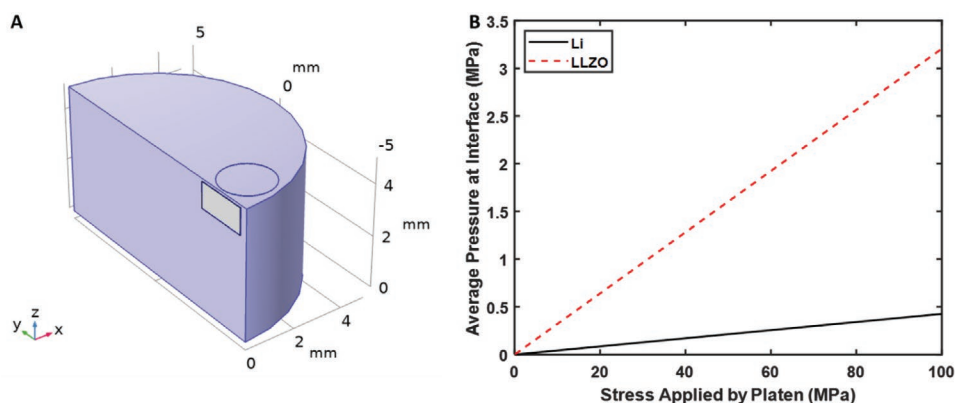


Figure 5. COMSOL Model of Experimental Configuration 1b for Li/LLZO system. a) Schematic of modeling domain for experimental configuration 1b. b) Average Developed Pressure at the interface in the Li electrode and LLZO solid electrolyte as a function of the Applied Stress.

primarily hydrostatic stress. We also model the mechanical state of a pellet in which only the electrolyte is undergoing compression, which results in significantly different pressures (and normal stresses) in the electrode versus electrolyte. Our conclusion that the mechanical state of the solid electrolytes in our study does not impact the equilibrium potential is a key point, and one that does not necessarily apply to systems that can develop composition variations. In addition to the scientific conclusions of this work, the results of this study are also relevant to the study of Li and Na metal penetration in solid electrolyte cracks or flaws during plating. In these cases, pressures on the order of 100s of MPa can develop, corresponding to a potential drop of 10s of mV, enough to strongly shift the current distribution.^[8] Further measurements and theoretical work carefully exploring the coupling of mechanics and electrochemistry in material sets relevant for solid state batteries is justified.

Acknowledgements

E.A.C. and M.J.W. contributed equally to this work. This work was supported by the U.S.-Israel Energy Center program managed by the U.S.-Israel Binational Industrial Research and Development (BIRD) Foundation and the U.S. Department of Energy (DOE) Office of Energy Efficiency and Renewable Energy (EERE) Vehicle Technologies Office (VTO) under contract DE-EE 00008855. The ideas in this work were significantly developed during the creation of the proposal that led to Award no. DE-SC0021070 from the U.S. Department of Energy, Office of Science, Office of Basic Energy Sciences. Y.S. contributed mechanical modeling and editing to this paper and was financially supported by this award.

Conflict of Interest

J.S. is the founder of Zakuro, Inc.

Data Availability Statement

The data that support the findings of this study are available from the corresponding author upon reasonable request.

Keywords

interfacial stress, interfacial thermodynamics, metal electrodes, solid state batteries

Received: April 30, 2021

Revised: May 27, 2021

Published online: June 16, 2021

- [1] P. Albertus, S. Babinec, S. Litzelman, A. Newman, *Nat. Energy* **2018**, 3, 16.
- [2] D. Aurbach, E. Zinigrad, Y. Cohen, H. Teller, *Solid State Ionics* **2002**, 3, 7207.
- [3] S. J. Harris, A. Timmons, W. J. Pitz, *J. Power Sources* **2009**, 193, 855.
- [4] X. B. Cheng, R. Zhang, C. Z. Zhao, Q. Zhang, *Chem. Rev.* **2017**, 117, 10403.
- [5] X. Zhang, Q. J. Wang, K. L. Harrison, K. Jungjohann, B. L. Boyce, S. A. Roberts, P. M. Attia, S. J. Harris, *J. Electrochem. Soc.* **2019**, 166, A3639.
- [6] E. G. Herbert, N. J. Dudney, M. Rochow, V. Thole, S. A. Hackney, *J. Mater. Res.* **2019**, 34, 3593.
- [7] R. Koerver, W. Zhang, L. De Biasi, S. Schweidler, A. O. Kondrakov, S. Kolling, T. Brezesinski, P. Hartmann, W. G. Zeier, J. Janek, *Energy Environ. Sci.* **2018**, 11, 2142.
- [8] B. Lu, Y. Song, Q. Zhang, J. Pan, Y. T. Cheng, J. Zhang, *Phys. Chem. Chem. Phys.* **2016**, 18, 4721.
- [9] P. Wang, W. Qu, W. L. Song, H. Chen, R. Chen, D. Fang, *Adv. Funct. Mater.* **2019**, 29, 1900950.
- [10] K. B. Hatzell, X. C. Chen, C. L. Cobb, N. P. Dasgupta, M. B. Dixit, L. E. Marbella, M. T. McDowell, P. P. Mukherjee, A. Verma, V. Viswanathan, A. S. Westover, W. G. Zeier, *ACS Energy Lett.* **2020**, 5, 922.
- [11] F. P. McGrogan, T. Swamy, S. R. Bishop, E. Eggleton, L. Porz, X. Chen, Y. M. Chiang, K. J. Van Vliet, *Adv. Energy Mater.* **2017**, 7, 1602011.
- [12] L. Porz, T. Swamy, B. W. Sheldon, D. Rettenwander, T. Frömling, H. L. Thaman, S. Berendts, R. Uecker, W. C. Carter, Y.-M. Chiang, *Adv. Energy Mater.* **2017**, 7, 1701003.
- [13] C. Monroe, J. Newman, *J. Electrochem. Soc.* **2004**, 151, A880.
- [14] A. K. Pannikatt, R. Raj, *Acta Mater.* **1999**, 47, 3423.
- [15] M. Ganser, F. E. Hildebrand, M. Klinsmann, M. Hanauer, M. Kamlah, R. M. Mcmeeking, *J. Electrochem. Soc.* **2019**, 166, H167.
- [16] L. Barroso-Luque, Q. Tu, G. Ceder, *J. Electrochem. Soc.* **2020**, 167, 070526.
- [17] A. Mistry, P. P. Mukherjee, *J. Electrochem. Soc.* **2020**, 167, 082510.
- [18] P. Barai, K. Higa, A. T. Ngo, L. A. Curtiss, V. Srinivasan, *J. Electrochem. Soc.* **2019**, 166, A1752.
- [19] Z. Ahmad, V. Viswanathan, *Phys. Rev. Lett.* **2017**, 119, 56003.
- [20] N. J. Taylor, S. Stangeland-Molo, C. G. Haslam, A. Sharafi, T. Thompson, M. Wang, R. Garcia-Mendez, J. Sakamoto, *J. Power Sources* **2018**, 396, 314.
- [21] M. Bay, M. Wang, R. Grissa, M. V. F. Heinz, J. Sakamoto, C. Battaglia, *Adv. Energy Mater.* **2020**, 10, 1902899.
- [22] J. Wolfenstine, J. L. Allen, J. Sakamoto, D. J. Siegel, H. Choe, *Ionics* **2018**, 24, 1271.
- [23] W. S. LePage, Y. Chen, E. Kazyak, K.-H. Chen, A. J. Sanchez, A. Poli, E. M. Arruda, M. D. Thouless, N. P. Dasgupta, *J. Electrochem. Soc.* **2019**, 166, A89.
- [24] A. Masias, N. Felten, R. Garcia-Mendez, J. Wolfenstine, J. Sakamoto, *J. Mater. Sci.* **2019**, 54, 2585.
- [25] A. Masias, N. Felten, J. Sakamoto, *J. Mater. Res.* **2021**, 36, 729.